

Magneto-optical traps for neutral atoms

B. N. Jagatap, K. G. Manohar, S. G. Nakhate, A. P. Marathe and S. A. Ahmad

Laser and Plasma Technology Division and Spectroscopy Division, Bhabha Atomic Research Centre, Trombay, Mumbai 400 085, India

We discuss here the basic principles of a magneto-optical trap, its characteristics and design considerations. We also present some of our work in the development of this trap.

AN ensemble of trapped atoms, at very low temperatures and high densities, is an ideal sample for a large variety of experiments¹. Applications of such samples range from very high resolution spectroscopy, metrology, nonlinear optics, atom interferometry to collision physics. Large optical thickness in such samples with negligible Doppler or collisional broadening allows significant improvement in the measurement of weak optical processes such as parity non-conserving transitions². In addition, a colder and denser atomic vapour is a good starting point to cross the phase boundary for the Bose-Einstein condensation (BEC) as has been demonstrated recently in the vapours of alkali atoms³⁻⁵.

One of the most efficient traps for neutral atoms is the magneto-optical trap (MOT) which is based on the scattering force in an inhomogeneous magnetic field⁶⁻¹⁴. MOT provides a simple and inexpensive way of obtaining large sample of cold and trapped atoms. It has a comparatively large trap depth which is relatively insensitive to experimental imperfections such as misalignments and polarization purity. It is capable of achieving densities as high as 10^{12} atoms/cm³ at a temperature down to a few micro Kelvin¹⁴. These characteristics have made MOT almost a standard and indispensable tool in experiments with laser cooled atoms ever since its experimental realization by Raab *et al.*⁶ in 1987. In the last ten years, there have been several investigations where this trap is used either as a source of cold atoms or to study the properties of the trap itself. In this article we discuss the ideas underlying these developments with special reference to our work in this area.

Radiation pressure on atom

Motion of a free atom subjected to interaction with a near-resonant laser light is described in terms of light forces¹⁵. There is a 'scattering force' or 'spontaneous radiation pressure force' that drives the atom in the direction of the light (axial force) and a 'gradient force' or 'dipole force' that pulls the atom into or out of the region of high light intensity (transverse force). The scat-

tering force is derived from the net recoil of the stimulated excitations followed by, on the average, isotropic spontaneous emissions and is strongly velocity dependent. The dipole force, in general, arises from the stimulated emission processes and can be considered as a force on an optically-induced dipole in the gradient of the optical electric field. It is directed along the intensity gradient and is dispersive in nature because of its dependence on the atomic polarizability.

Initial attempts to form neutral atom traps were based on the gradient force. In such traps, atoms are pulled into or out of the region of the high light intensity depending on whether the laser frequency is tuned below or above the selected atomic resonance. To obtain large dipole force, one has to balance the effect of detuning from exact resonance and the amount of saturation for a given laser power. One of the basic limitations of the dipole traps comes from the large saturation parameter required for confinement. For example¹⁵, to have a dipole trap as deep as 10^{-4} eV for Na atoms, one needs to have laser power of ~ 1 W. A potential of this depth is capable of confining atoms moving with velocity of 2×10^3 cm/s. For lower laser powers, the dipole traps will turn out to be very shallow.

The scattering force, on the other hand, has led to the useful concept of optical cooling of atoms by a laser tuned below the atomic resonance¹⁶. For a laser of frequency ω_L propagating in \pm direction and interacting with a two level atom of transition frequency ω_a , the average scattering force, F_{\pm} , is calculated in terms of the photon momentum $\hbar k$ and the average rate of photon absorption

$$F_{\pm} = \pm \hbar k \frac{\gamma}{2} \frac{s}{1 + s + [2(\delta \mp kv)/\gamma]^2}, \quad (1)$$

where v is the velocity of the atom, k is the wave vector, $\delta = \omega_L - \omega_a$ is the detuning of the laser frequency from the atomic resonance, γ is the spontaneous decay width of the atomic excited state and $s = I/I_0$ is the saturation parameter. Here I is the intensity of the laser beam and I_0 is the saturation intensity. This force provides the viscous drag force in the optical molasses¹⁶. However the scattering force by itself cannot form a trap. By trapping, we mean confining a particle or collection of them to a region of space by a position-dependent force. In that sense, the scattering force, which is merely velocity dependent, can not form a trap. Realization of a trapping

scheme using the scattering force alone is ruled out by the optical Earnshaw theorem¹⁷ (OET) which, in analogy with the Earnshaw theorem in the electrostatics, states that it is impossible to trap a small dielectric particle at a point of stable equilibrium in free space by using only the scattering force of the radiation pressure. This is merely a consequence of the fact that the divergence of the scattering force is identically equal to zero. The difficulty posed by the OET can be circumvented by introducing a spatially varying magnetic field to exploit the internal structure of the atom, in conjunction with the scattering force. Such a hybrid trapping device which uses both magnetic and optical fields is called a magneto-optical trap (MOT) or Zeeman Optical Trap (ZOT).

Principle of MOT

The basic principle^{6,7} of a MOT is illustrated in Figure 1 by considering a hypothetical two level atom with $|J_g = 0\rangle$ ground state and $|J_e = 0\rangle$ excited state placed in a weak inhomogeneous magnetic field $B_z(z) = Az$. Energy levels of the atom are Zeeman split by such a linearly varying magnetic field by an amount $\Delta E = \mu_B g_J m_J A z$, where μ_B is the Bohr magneton, m_J is the magnetic quantum number and g_J is the Landé g factor of the level having angular momentum J . The atom is illuminated by two counter-propagating laser beams of frequency ω_L and of polarization σ^+ and σ^- propagating in the $+\hat{z}$ and $-\hat{z}$ directions respectively. The laser beams are detuned below the zero field atomic resonance by $|\delta| > \gamma$. Note here that as per the electric dipole selection rules, the σ^+ and σ^- beams drive the transitions $|m_g = 0\rangle \rightarrow |m_e = 1\rangle$ and $|m_g = 0\rangle \rightarrow |m_e = -1\rangle$ respectively. Atomic resonance then occurs only near two points $z = \pm z'$ where the laser frequency is in resonance with the Zeeman tuned atomic states. Consequently, an atom at $z = +z'$ will absorb photon

preferentially from σ^- beam and will experience a scattering force in the $-\hat{z}$ direction. On the other hand, an atom at $z = -z'$ will absorb photons mostly from the σ^+ beam and will be driven in the $+\hat{z}$ direction. In effect, the atom will experience a net time averaged force towards the origin. The turning points $\pm z'$ can be moved by either tuning the laser or changing the magnetic field gradient. Having the laser beams tuned to the red of the resonance also provides the damping force.

For a moving atom, the Doppler effect changes the resonance condition by shifting the optical frequencies in the rest frame of the atom. For example, in Figure 1, an atom moving in the $+\hat{z}$ direction will see σ^- laser beam blue shifted and the resonance will occur at some $z'' < z'$. On the other hand, the same atom will see the σ^+ laser beam red shifted and the resonance condition will not be satisfied anywhere on the z axis. In general for a given velocity v of the atom, the Zeeman and Doppler shifts combine to produce resonance with the σ^\pm beams when $\delta = \pm(kv + \mu_A z/\hbar)$. The interior region between $\pm z'$ permits resonance over an extended velocity range as the atom moves in the inhomogeneous magnetic field. The atom, thus can absorb only from a laser beam counter-propagating to its own motion and experiences a net force towards the origin.

The trapping scheme of a MOT as discussed above can be readily generalized to three dimensions. Such an extension involves six laser beams propagating in the $\pm\hat{x}, \pm\hat{y}$ and $\pm\hat{z}$ directions and a spherical quadrupole magnetic field. The polarizations of the laser beams are organized in such a way that every counter-propagating pair has beams of opposite helicity. The spherical quadrupole field is produced by a pair of coils in 'Maxwell configuration' as described later. Furthermore, the trapping scheme can be generalized to atomic transitions involving more complex angular momentum states as observed in the alkali atoms.

MOT characteristics

MOT provides a relatively deep static trap for neutral atoms at very reasonable intensities of laser beams as may be seen from a simple estimate⁷. From eq. (1), we find that the maximum scattering force acting on an atom is

$$F_{\max} = \hbar k \frac{\gamma}{2} \frac{s}{(s+1)} \quad (2)$$

An atom with kinetic energy less than $2rF_{\max}$ can be stopped and contained in a MOT of size $2r$ ($r = z'$ in 1-D example of Figure 1) when $|\delta| > \gamma_s$, where $\gamma_s = \gamma\sqrt{1+s}$ is the saturation broadened homogeneous linewidth. Equating $2rF_{\max}$ with the thermal energy $3K_B T_0/2$, we find that the depth of a MOT is

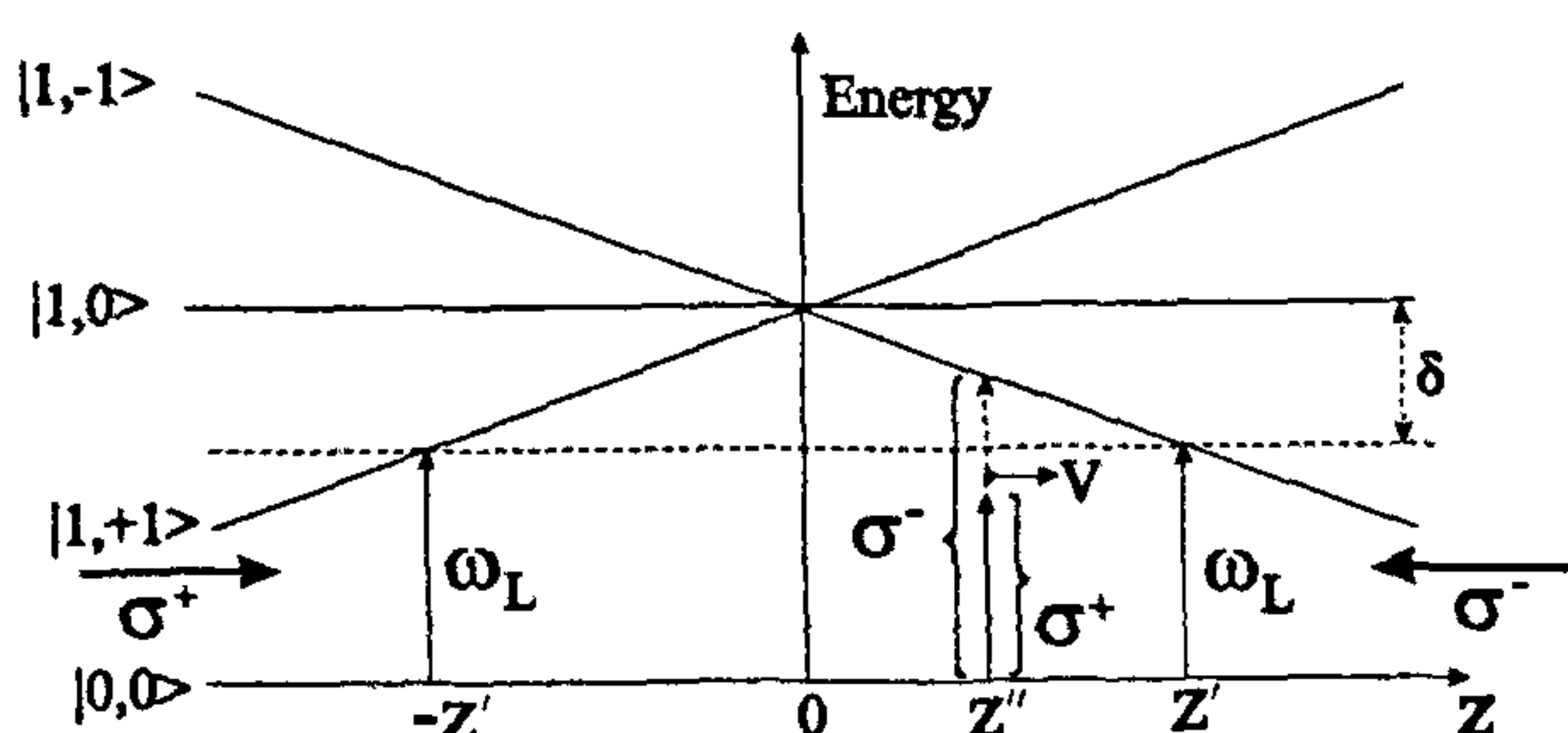


Figure 1. Working principle of MOT in one dimension. Inhomogeneous magnetic field gives rise to space dependent Zeeman splitting. $|J, M\rangle$ denote the Zeeman states. Counter propagating laser beams of frequency ω_L and polarization σ^+ and σ^- (shown by arrows) produce space dependent force on the atom which is directed towards the origin. At $z = z''$ an atom moving to the right with velocity V sees σ^+ beam red shifted and σ^- beam blue shifted.

$$T_0 = \frac{4F_{\max}r}{3K_B} \quad (3)$$

For example, for Cs atom with trap dimensions of a few mm, a trap depth of the order of 1 K can be conveniently achieved with laser intensity of 2–3 mW/cm² ($I_0 = 2.3$ mW/cm² for Cs). We may compare this with the intensity requirement for a dipole trap of similar depth.

In the first demonstration of MOT, Raab *et al.*⁶ trapped about 10^7 atoms. The atoms were first precooled by slowing an atomic beam to velocities ~ 20 m/s before they were captured. Monroe *et al.*⁹ have shown that the atoms can be trapped without the precooled step by embedding the MOT in a vapour cell. In this case the MOT captures the atoms directly from the low velocity tail of the thermal distribution. In such a vapour cell trap, they could trap about 1.8×10^7 atoms in a few seconds. The number of atoms N in a MOT is determined by a balance between the capture rate R into the trap and the loss rate from the trap^{9–12}. The loss rate is governed by the collisions of various kinds involving ground and excited states of the atoms in the trap and the background gas. In general the rate equation describing the number of atoms in a MOT may be written as

$$\frac{dN}{dt} = R - \frac{N}{\tau} - \beta N^2, \quad (4)$$

where τ is the lifetime of an atom to remain in the trap. The lifetime is usually governed by collisions with the background gas which knock out atoms out of the trap. The third term on the right (eq. (4)) represents the loss resulting from two-body collisions between the atoms in the trap. These collisions are significant only at high densities of the trapped atoms.

The loading rate R depends on the method adopted to load the MOT. As mentioned earlier, the simplest loading method is to form a trap in a low pressure vapour of atoms to be trapped. In this case, we may start with the assumption that the trap catches all the atoms that enter the trapping region with a velocity less than the maximum capture velocity v_c . Typically the value of v_c is the velocity of atom¹¹ that is stopped by a force equal to half the maximum scattering force, F_{\max} . Thus, we have $v_c = \sqrt{2F_{\max}r/m}$, where m is the mass of the atom and as before r is the radius of the trap. For example, for Cs atoms at a saturation parameter $s > 1$ and for trap radius of 4 mm, $v_c \sim 15$ m/s. In order to calculate the flux of such atoms entering the trap, we may employ the kinetic theory of gases to obtain

$$N = R\tau \sim \frac{1}{5} \left(\frac{v_c}{\bar{v}} \right)^4 \frac{A}{\sigma} \quad (5)$$

where $\bar{v} = \sqrt{8k_B T / \pi m}$ is the average speed of the background vapour, A is the surface area of the trapping region and σ is the cross section for collisions with the background gas. Using typical collision cross section $\sigma \sim 2 \times 10^{-13}$ cm² for Cs, with $r = 4$ mm and $v_c = 15$ m/s, one finds at room temperature $N \sim 10^7$ which is the order of magnitude of the number of atoms trapped in a MOT.

The lifetime of the atoms in the MOT may be shown¹¹ to be given by

$$\tau = \frac{(\pi m k_B T / 8)^{1/2}}{\sigma P} \quad (6)$$

For example, in a background of Cs atoms at room temperature and at a pressure of 10^{-8} torr, $\tau \sim 1$ s. From eqs (5) and (6), it is important to note that the number of atoms in the MOT is independent of the pressure in the vapour cell. This allows one to work at room temperature vapours of Rb and Cs where the vapour pressures at 300 K are 3.3×10^{-7} torr and 1.67×10^{-6} torr respectively.

There are two processes which limit the density of the atoms in a MOT. The first process corresponds to the two-body collisions between the ground and excited state atoms in the trap. In these collisions, a part of the excitation energy is transferred into the kinetic energy, resulting in the trap loss. Experiments⁸ have shown that the value of $\beta \sim (1-5) \times 10^{-11}$ cm³/s, which sets up a limit of 10^{11} for the density of atoms. The second process corresponds to the reabsorption of fluorescence photons by the atoms which results in the repulsive forces between the atoms¹⁴. In other words, at certain densities, the outward radiation pressure of the fluorescent light balances the confining force of the trapping beams. Further increase in the number of trapped atoms leads to larger atomic clouds but not to higher number densities. In some cases the radiation pressure may cause the sample to break into a central cloud surrounded by an orbiting ring¹⁰.

Design considerations

A MOT consists of three major subsystems: a UHV chamber with a source of atoms to be trapped, a spherical quadrupole magnetic field and lasers/optics systems. The need for UHV ($\sim 10^{-8}$ torr) stems out of the considerations of the average lifetime of the trapped atoms and has been discussed earlier. Since it is possible to capture atoms directly from the low pressure vapour of the atoms, the chamber can be a simple vapour cell made of fused silica. A fused silica vapour cell designed and fabricated in our laboratory is shown in Figure 2a. The cell is essentially a 'double' cross having six arms in the

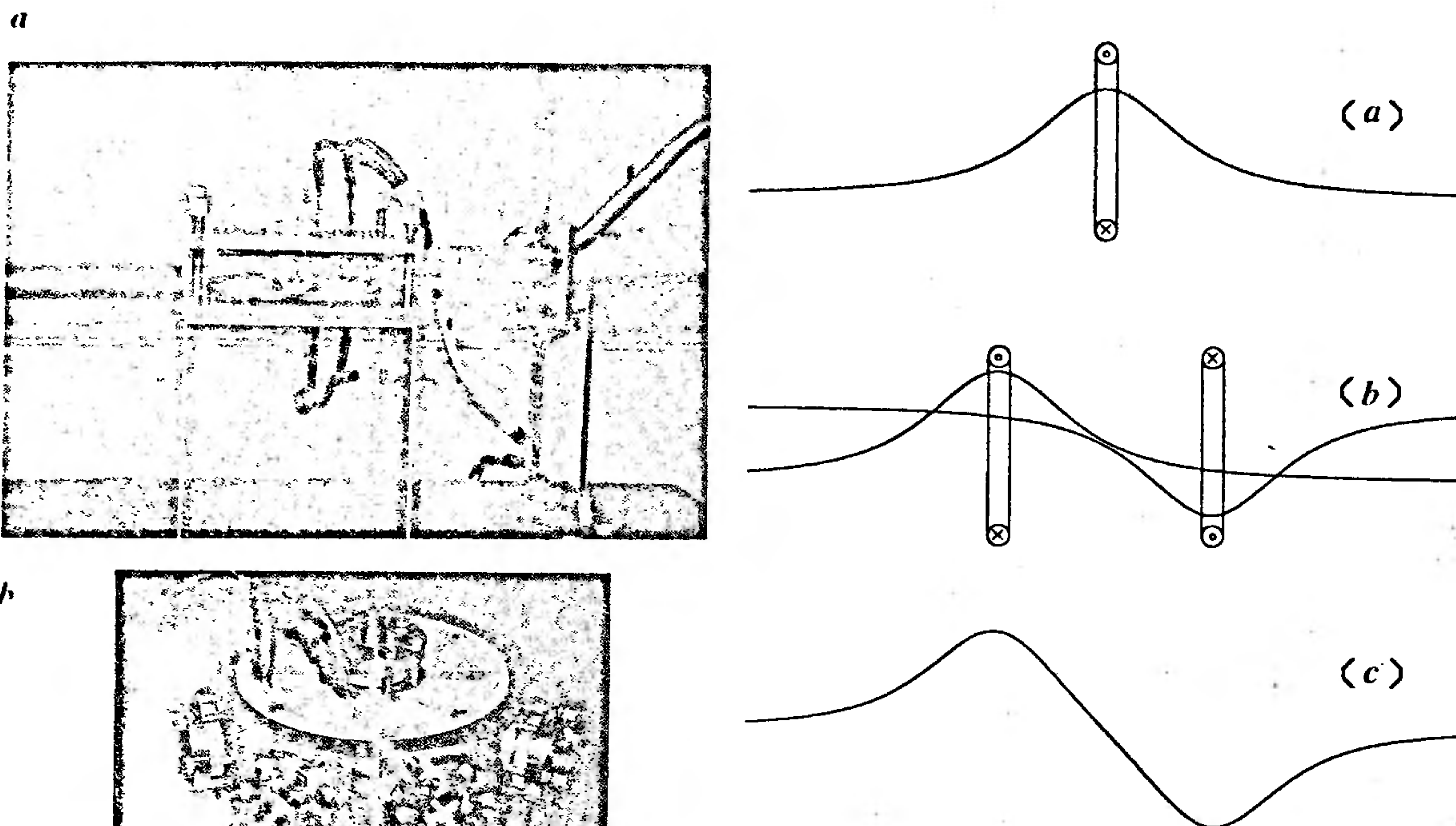


Figure 2. *a*, MOT with a glass vapour cell installed in BARC. It is mounted on an indigenously built vibration isolation platform. *b*, MOT with a stainless steel vapour chamber designed and fabricated in BARC.

$\pm x$, $\pm y$, $\pm z$ directions. Each arm is about 12 cm in length and is fused with a window of 2.5 cm dia. The vapour cell has a port connecting to a UHV system consisting of an ion pump (24 l/s) and a turbo molecular pump (150 l/s). A reservoir of Rb/Cs is attached to the chamber. In our vapour cell, we have provided two optical ports for observation of cooled and trapped atoms. Although a simple glass device such as shown in Figure 2*a* can be used to demonstrate trapping of atoms, a stainless steel (SS) chamber is desirable for better results. Usually the lifetime of the trapped atoms in a glass vapour cell is shorter compared to the atoms trapped in a SS chamber⁹. This difference is due to the diffusion of He and H₂ through the glass surface which increases the background pressure. In Figure 2*b* we have shown a SS MOT chamber designed and fabricated in our labora-

Figure 3. Schematic representation of magnetic field produced by a two-coil configuration. *a*, z component of B due to a single coil; *b*, z component of B due to two identical coils with spatial separation $D = 1.25 R$ and carrying opposite currents; *c*, z component of the quadrupole field along the axis. R is the radius and D is the separation between the coils.

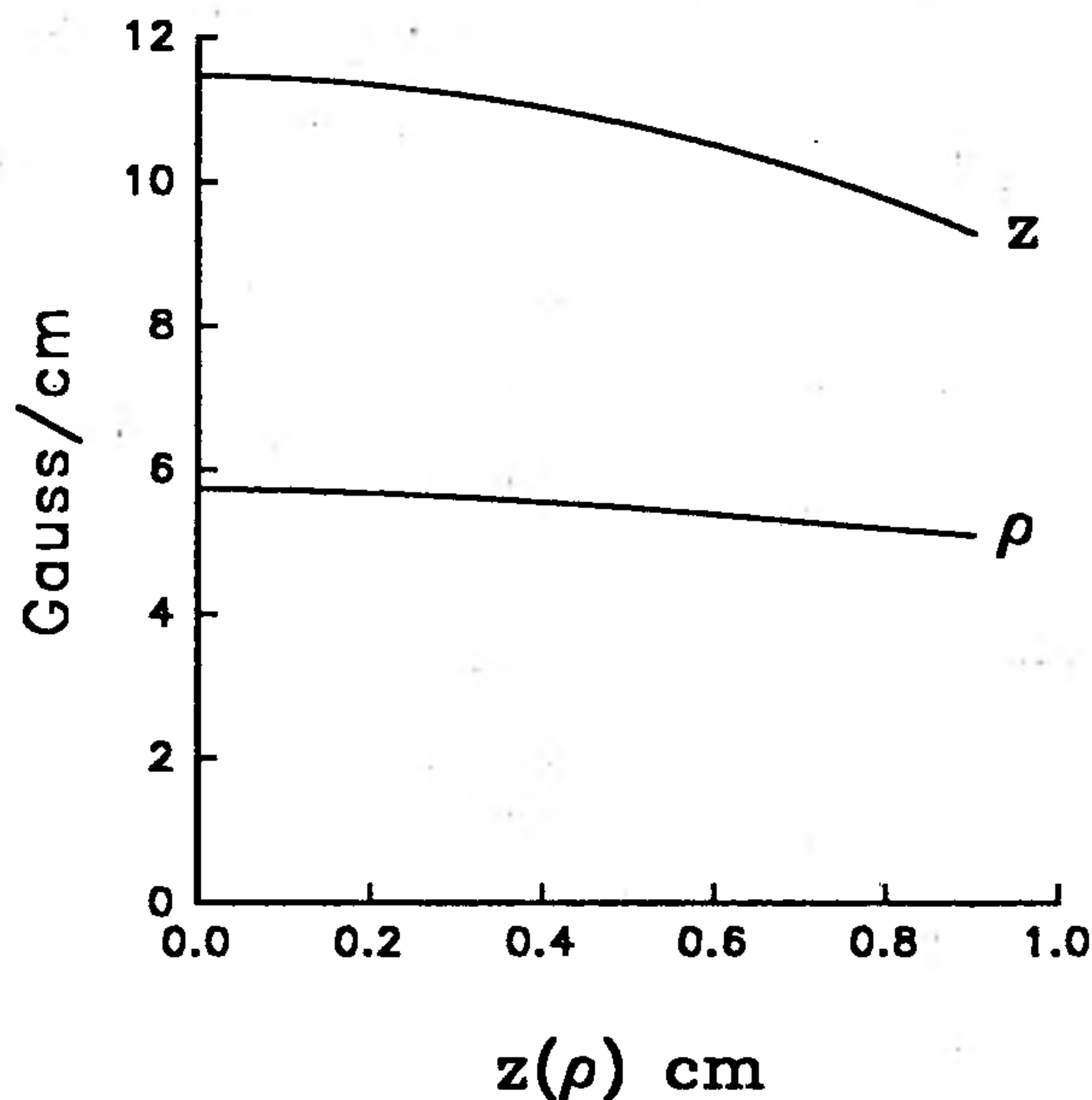


Figure 4. Magnetic field gradient along the axial (z) and radial (ρ) directions for a two coil configuration excited by 100 ampere turns. Identical coils are of $R = 30$ mm and $D = 37.5$ mm.

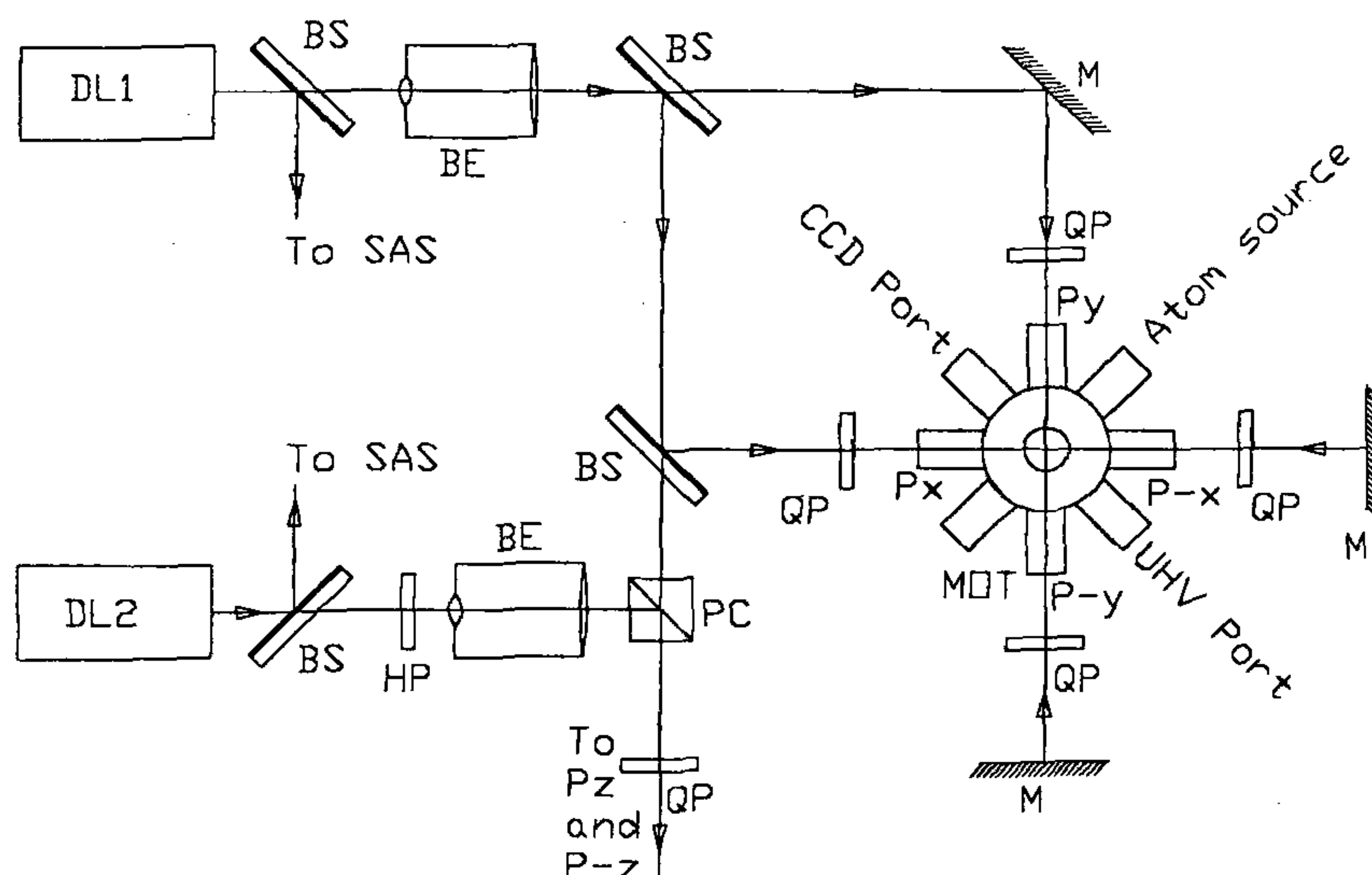


Figure 5. Optical lay-out for the trapping experiment in a MOT. DL_1 and DL_2 are diode lasers for trapping and hyperfine pumping respectively. The trapping beams pass through the six optical ports denoted by $P_{\pm x}$, $P_{\pm y}$ and $P_{\pm z}$. SAS denotes saturated absorption spectroscopy. BS = beam splitter, BE = beam expander, QP = quarter wave plate, M = mirror, H = half wave plate and PC = polarizing beam combiner.

tory. Out of the ten ports provided in this assembly, six ports along the Cartesian axes are used for passing the trapping beams, one port is for connecting to the UHV system, one port for connecting a Cs/Rb reservoir and two ports for observations through CCD and fluorescence.

Spherical quadrupole magnetic field is provided by two coils carrying opposite currents and mounted appropriately on the UHV chamber. In Figure 3, we show how such a configuration involving two identical coils of radius R and separated by a distance D gives rise to a quadrupole field. In our experiments, the coils are of 30 mm radius. Such a coil configuration may be analysed theoretically using polynomial expansion method to obtain the working parameters. Required magnetic field gradient for MOT is typically in the range of 5–15 G/cm. In Figure 4, we show the variation of the gradient in the axial and radial directions as a function of distance when the quadrupole magnet is excited by 100 ampere turns. We see here that the gradient is nearly constant over a small distance of about 5 mm. This region essentially forms the trapping region in the MOT.

For trapping of Rb ($\lambda = 780$ nm) and Cs ($\lambda = 852$ nm) atoms, low power diode lasers with bandwidth of ~ 1 MHz are sufficient. Owing to the large absorption cross-section at these wavelengths, the saturation intensities are in the range of 2–4 mW/cm². It is desirable to have a large diameter d for the trapping beams since the loading rate increases rapidly with d . This may be seen from eq. (5) where both the capture velocity and

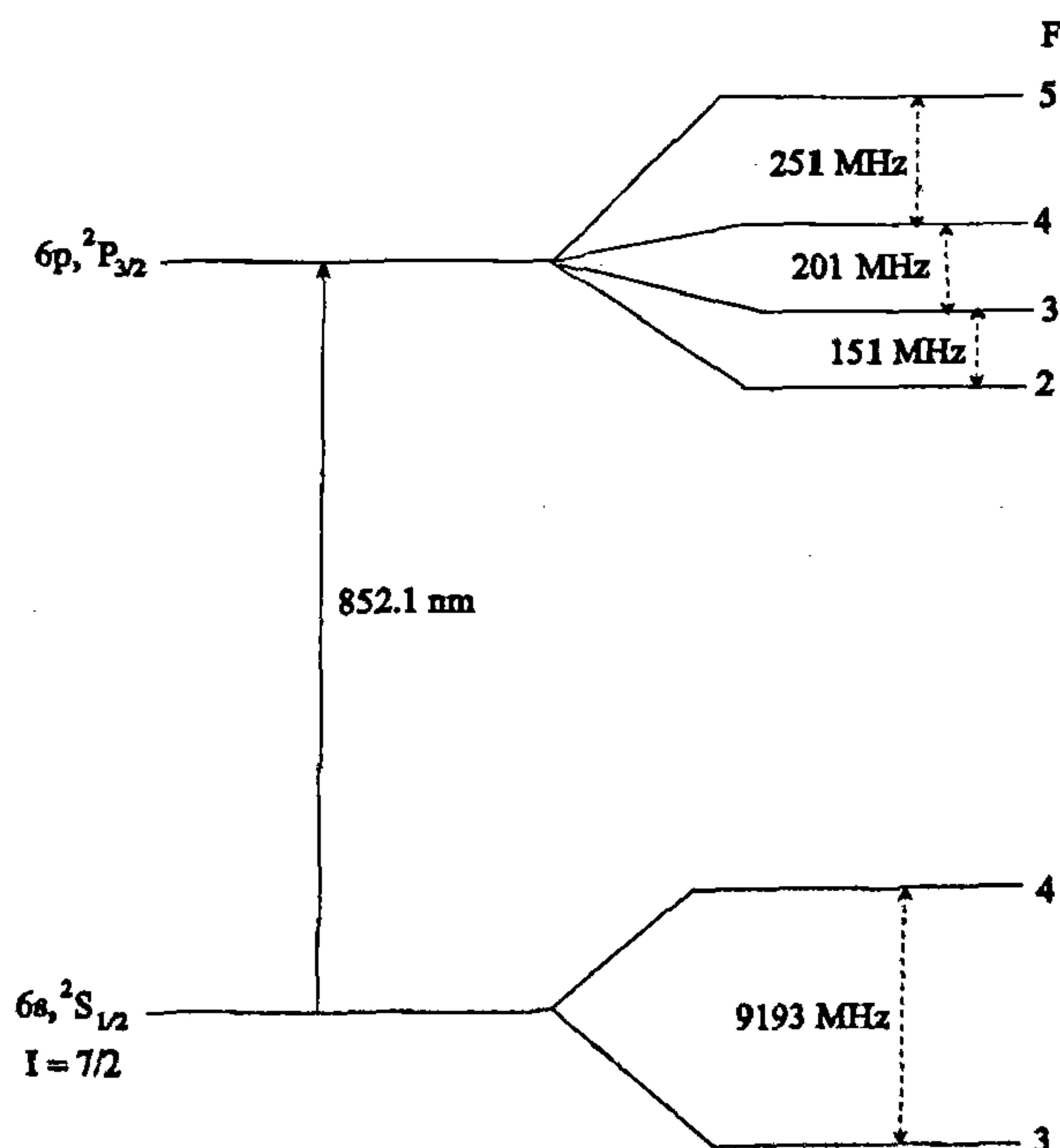


Figure 6. Energy level diagram of ^{133}Cs relevant to trapping in a MOT.

the area of the trap are functions of the d . The overall dependence may be shown to be d^4 which is close to the

$d^{3/6}$ dependence observed experimentally¹³. In our experiments, we plan to use $d = 1-2$ cm. A detailed optical lay out for MOT is shown in Figure 5. The laser output is polarized and split into three circularly polarized beams of $3-4$ mW/cm². Each of these beams enter and exit the MOT chamber along the three orthogonal axes, pass through the quarter wave plates and then get retroreflected. Energy level diagram of Cs is shown in Figure 6. The transition $6S_{1/2}F = 4 \rightarrow 6P_{3/2}F = 5$ is the trapping transition. The trapping laser is locked to the red of this transition using saturated absorption spectroscopy. Usually a detuning of $15-30$ MHz is provided depending on the magnetic field gradient. Due to non-resonant spontaneous Raman process, $F = 3$ ground state is usually populated during the trapping process. In order to prevent the atoms from accumulating in the $F = 3$ state, a second laser corresponding to the transition $6S_{1/2}F = 3 \rightarrow 6P_{3/2}F = 4$ is used. This hyperfine pumping laser is locked using saturated absorption spectroscopy and sent through one of the ports of the MOT overlapping with the trapping region formed by the trapping beams.

Conclusions

Laser cooling and trapping of atoms is a very active area of research encompassing a wide spectrum of problems in physics. MOT is a vital component in all these investigations. It provides a simple and inexpensive way of obtaining a large number of cold and trapped atoms. Densities of the order of 10^{11} atoms/cm³ and trap depths of < 1 K can be conveniently obtained using this device. There exist a number of variants of MOT which are used in specific applications. For example, when high atom densities (10^{12} atoms/cc) are desired, a MOT with a dark spot is used¹⁴. In this variety of MOT, the hyperfine repumping laser is tailored spatially to confine the atoms predominantly in the 'dark' hyperfine level ($6S_{1/2}F = 3$ in Figure 6) that does not interact with the trapping laser beams. Although a six-beam trapping geometry is a standard configuration, there also exists a four-beam geometry where the laser beams are organized in a tetrahedral configuration¹⁸. Such a design may offer advantages in certain applications.

We have undertaken a major programme on laser cooling and trapping of atoms in BARC¹⁹. Development of the MOT is a part of this intensive programme. While

much of the stress in the initial phase of this programme is on developing facilities for laser cooling and trapping for ultra high resolution spectroscopy, major objectives of our programme are to study the collective behaviour of fundamental quantum systems and initiate studies related to atom optics over the next few years. Needless to say that MOT and some of its variants will be the work horses in this programme.

1. See for example, Kasevich, M., Moler, K., Riis, E., Sundermann, E., Weiss, D. and Chu, S., *At. Phys.*, 1991, **12**, 47-57.
2. Stacey, D. N., *At. Phys.*, 1993, **13**, 46-61.
3. Anderson, M. H., Ensher, J. R., Matthews, M. R., Wieman, C. E. and Cornell, E. A., *Science*, 1995, **269**, 198-201.
4. Davis, K. B., Mewes, M. O., Andrews, M. R., van Druten, N. J., Durfee, D. S., Kurn, D. M. and Ketterle, W., *Phys. Rev. Lett.*, 1995, **75**, 3969-3973.
5. Bradley, C. C., Sackett, C. A., Tollet, J. J. and Hulet, R. G., *Phys. Rev. Lett.*, 1995, **75**, 1687-1690.
6. Raab, E. L., Prentiss, M., Cable, A., Chu, S. and Pritchard, D., *Phys. Rev. Lett.*, 1987, **59**, 2631-2634.
7. Metcalf, H., *J. Opt. Soc. Am.*, 1989, **B6**, 2206-2210.
8. Sesko, D., Walker, T., Monroe, C., Gallagher, A. and Wieman, C., *Phys. Rev. Lett.*, 1989, **63**, 961-964.
9. Monroe, C., Swann, W., Robinson, H. and Wieman, C., *Phys. Rev. Lett.*, 1990, **65**, 1571-1574.
10. Sesko, D., Walker, T. and Wieman, C., *J. Opt. Soc. Am.*, 1991, **B8**, 946-951.
11. Stean, A. M., Chowdhury, M. and Foot, C. J., *J. Opt. Soc. Am.*, 1992, **B9**, 2142-2158.
12. Gibble, K. E., Kasapi, S. and Chu, S., *Opt. Lett.*, 1992, **17**, 526-528.
13. Lindquist, K., Stephens, M. and Wieman, C., *Phys. Rev.*, 1992, **A46**, 4082-4090.
14. Ketterle, W., Davis, K. B., Joffe, M. A., Martin, A. and Pritchard, D., *Phys. Rev. Lett.*, 1993, **70**, 2253-2256.
15. Ashkin, A., *Science*, 1980, **210**, 1081-1088.
16. Lett, P. D., Phillips, W. D., Rolston, S. L., Tanner, C. E., Watts, R. N. and Westbrook, C. I., *J. Opt. Soc. Am.*, 1989, **B6**, 2084-2107 and references therein.
17. Ashkin, A. and Gordon, J. P., *Opt. Lett.*, 1983, **8**, 511-513.
18. Shimizu, F., Shimizu, K. and Takuma, H., *Opt. Lett.*, 1991, **16**, 339-341.
19. Jagatap, B. N., Ahmad, S. A., Chatterjee, U. K. and Roy, A. P., in *Physics with Cooled and Trapped Atoms and Ions*, BARC, 1998; Jagatap, B. N. and Ahmad, S. A., *Phys. News*, 1997, **28**, 83-96.

ACKNOWLEDGEMENTS. We thank Dr A. P. Roy, Head, Spectroscopy Division, BARC for his keen interest in this work and for valuable suggestions. Many discussions with Dr R. C. Sethi are gratefully acknowledged. Thanks are due to Technical Physics and Prototype Engineering Division for fabricating the quartz cell shown in Figure 1a.